JOURNAL OF SOLID STATE CHEMISTRY 42, 11–21 (1982)

The Transition from Spinel-Type Structure to Rocksalt-Type Structure in the Compound $CdHo_2S_4$, as Observed by Electron Microscopy/Diffraction

M. BAKKER,* F. H. A. VOLLEBREGT, AND C. M. PLUG

Gorlaeus Laboratories, State University, P.O. Box 9502, 2300 RA Leiden, The Netherlands

Received July 22, 1981; in revised form October 27, 1981

At a temperature above 1173 K the spinel-type structure of $CdHo_2S_4$ becomes unstable and gradually transforms into a rocksalt-type structure. During transition both Cd^{2+} and Ho^{3+} cations shift. Electron diffraction patterns obtained during transition show that the Cd, which shifted from a tetrahedral to an octahedral site, distorts the sulfur lattice. This distortion becomes visible as a modulation of the sulfur matrix. The modulation originally occurs in many crystallographic directions, however, upon annealing the ⟨111⟩ direction becomes preferred. Small domains of the high-temperature structure of $CdHo_2S_4$ appear to occur also in samples that were annealed well below 1173 K for a long period.

Introduction

The well-known structure of the mineral "spinel" has been observed for many ternary oxides and sulfides (*1, 2*). In the simplest cases the spinel structure is adopted with A^{2+} and B^{3+} cations occupying $\frac{1}{8}$ of the tetrahedral and $\frac{1}{2}$ of the available octahedral sites in a cubic close-packed X^{2-} anion lattice. Depending on the cation radii the anion lattice can deform, making the octahedra smaller and at the same time the tetrahedra larger (the anion parameter x can change from 0.375 to 0.390). The coordination is mostly not ideal in this structure, and the geometry is, as the charges are completely compensated around the X anion according to "Pauling's rule" (*3*). Each X is surrounded by three B^{3+} in 6-coordination and one A^{2+} in 4-coordination. More complex spinel-type structures also occur: so-called inverse or partly inverse spinel. In these structures the occupation of the tetrahedral and octahedral sites by A^{2+} and B^{3+} can vary. In completely inverse spinel the tetrahedral site is occupied by B^{3+} and the tetrahedral sites by A^{2+} and B^{3+}. It is worth noting that the condition of charge compensation is less strict in sulfur compounds than in oxygen compounds due to the polarizability of sulfur.

A number of sulfospinels are formed with Cd^{2+} or Mn^{2+} and several trivalent rare earth cations. The radius ratio of the cations, together with the possible deformation of the sulfur lattice, determines to a large extent whether the spinel-type structure is adopted. For example, compounds $MnRE_2S_4$, with RE = Tm, Yb, and Lu, and compounds $CdRE_2S_4$, with RE = Ho, Y, Er, Tm, Yb, and Lu, all crystallize in a spinel-type structure (*1, 2, 4*). In the latter compounds the radius of the Ho^{3+} cation limits the stability of the spinel-type struc-

* To whom correspondence should be addressed.

0022-4596/82/040011-11$02.00/0

ture. When Ho^{3+} is replaced by the slightly larger Dy^{3+} the compound adopts the Th_3P_4-type structure (*5*). X-Ray diffraction studies report the structure of $CdHo_2S_4$ as that of a normal spinel with a lattice parameter a_{sp} = 11.167 or 11.168 Å (*6, 7*). However, one X-ray diffraction study reports a lattice parameter a_{sp} = 11.24 Å (*8*) and suggests the structure to be that of an "intermediate" spinel, meaning that for this compound only 60% of the Cd^{2+} is occupying a tetrahedral site. It should be pointed out that this study does not claim any inverse character for the structure. This implies that the remaining 40% of the tetrahedral sites are vacant and thus not occupied by Ho^{3+}. In order to clarify the noted discrepancies a number of $CdHo_2S_4$ samples were heated to different temperatures and examined by means of powder X-ray diffraction and electron microscopy diffraction.

Experimental

CdS and Ho_2S_3 were prepared by heating the oxides contained in graphite crucibles using a h.f. induction furnace in a stream of H_2S gas. The diffraction patterns of the sulfides were recorded on a Philips powder diffractometer (Cu$K\alpha$, λ = 1.5418 Å). Equimolar mixtures of CdS and Ho_2S_3 were similarly heated between 1173 and 1373 K for 2 hr and air-quenched. Also, a mixture was heated to 1173 K and annealed at 973 K for 2 weeks. Finally, one sample was kept for 24 h at 1173 K and air-quenched. After examination by X-ray diffraction the samples were crushed, dispersed in alcohol, and mounted on a 400-mesh copper grid, coated with Formvar/carbon holey film. These were examined in a Siemens Elmiskop 102 fitted with a double tilt and lift cartridge and operating at 100 and 125 kV. To be able to determine lattice constants from electron micrographs, the camera length λL was calibrated versus the objective current using an Al film. Images were recorded on Kodak electron image plates and developed for 7 min in D19.

Results

a. X-Ray Powder Diffraction

The powder diffraction results for the heated samples clearly show the effect of temperature treatment. The diffraction patterns indicate that besides a $CdHo_2S_4$ spinel-type phase a second phase is also formed. This second phase appears to be $CdHo_4S_7$.[1] The enrichment in Ho is a result of evaporation of CdS at the operating temperature of 1173 K. The lattice parameter for $CdHo_2S_4$ annealed at 973 K was calculated from the powder pattern: a(spinel) = 11.17(1) Å. In the other powder patterns peaks from $CdHo_2S_4$ broaden and an increase in background is observed as the heating temperature increases. The spinel lattice parameter obtained from these powder patterns, however, remains the same.

b. Electron Microscopy/Diffraction

Three types of sample, all with composition $CdHo_2S_4$ but different in heat treatment, were examined using a double tilt and lift device in the electron microscope. From all samples a large number of different reciprocal lattice sections and corresponding micrographs (bright and dark field) were obtained. The most relevant ones follow.

1. Sample heating: temperature T = 973 K for 2 weeks. The selected area diffraction pattern in Fig. 1a shows a ⟨110⟩ reciprocal lattice section of a crystal with a spinel-type structure: a(spinel) = 11.15(5) Å. Other lattice sections could also be indexed using a

[1] The structure of $CdHo_4S_7$ is monoclinic, $C2/m$. It is isostructural with Y_5S_7 (*9*) and can be described as mimetic twinned c.c.p. The $d(001)$ spacing is thus approximately $7 \times d(113)_{c.c.p.}$ (*10*). The unit cell parameters are a = 12.75, B = 3.81, c = 11.45 Å., β = 105.63° (*2*).

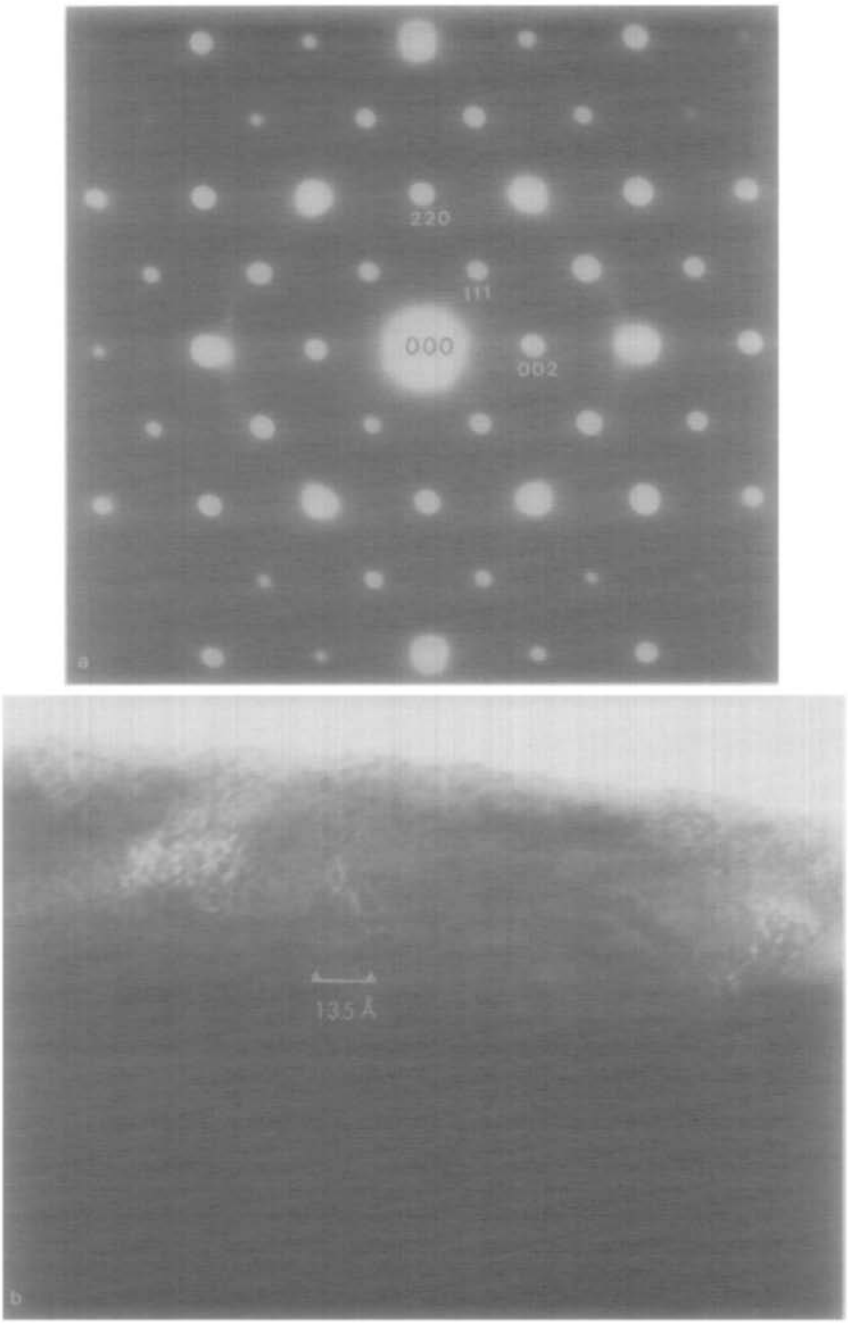

FIG. 1. (a) A ⟨110⟩ reciprocal lattice section of a crystal with composition $CdHo_2S_4$ and heated at 973 K for 2 weeks. Indices refer to a spinel-type unit cell. (b) Micrograph of a similar crystal. In the thinner region of the crystal, domains extend over 20 Å.

spinel-type unit cell. Micrographs from most crystals show a rather inhomogeneous contrast in both bright and dark field. In some crystals, however, small regions containing domains can be observed. For example, in Fig. 1b in the thinner part of the crystal the domains are approximately 20 Å.

2. Sample heating: 1173 K < T < 1373 K for 2 hr. Samples now are in a transition state, which can be seen from the diffraction patterns in Fig. 2. In Fig. 2a, which is indexed using a NaCl-type unit cell ($a = \frac{1}{2}$ a(spinel)) with a lattice parameter a = 5.65(3) Å, diffuse scattering can be observed besides the Bragg reflections. The

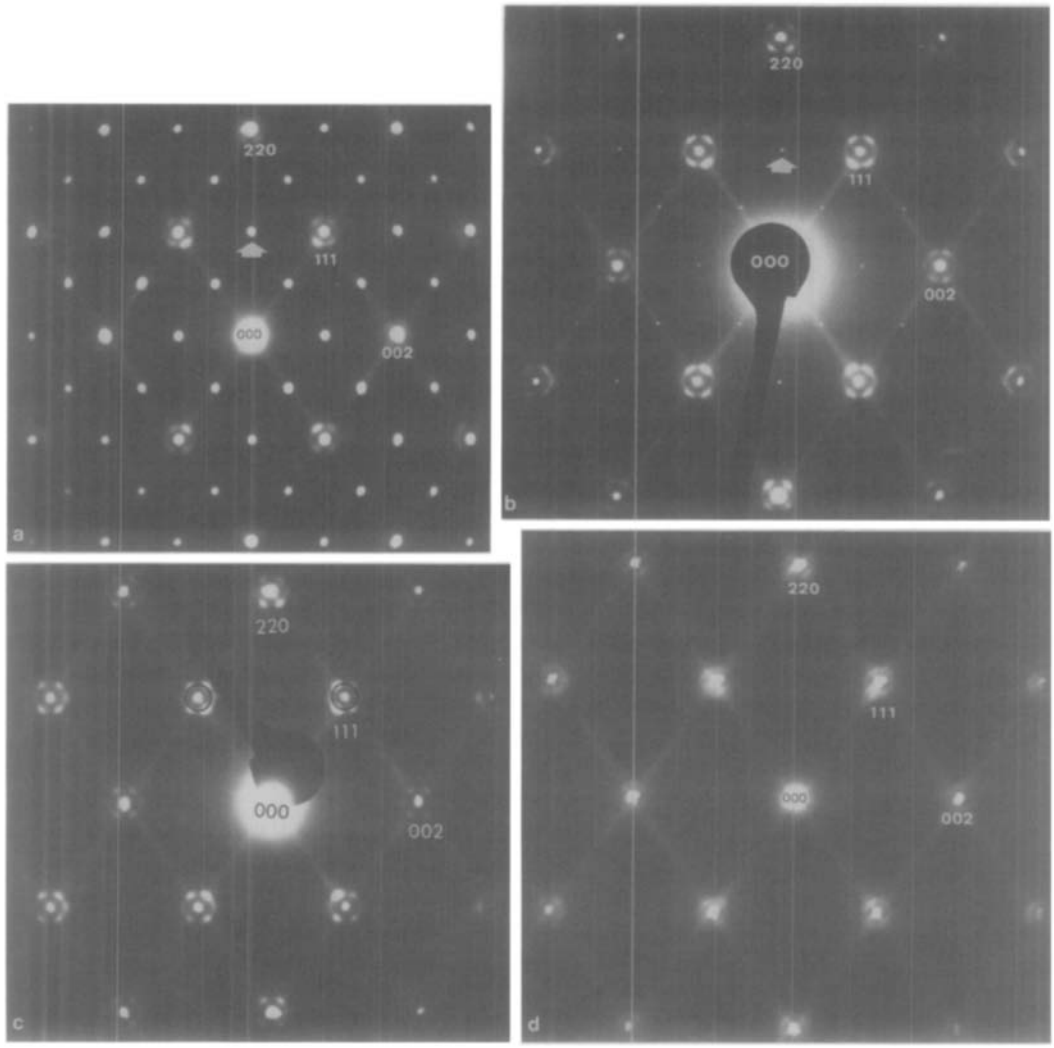

FIG. 2. (a–c) ⟨110⟩ Reciprocal lattice sections of $CdHo_2S_4$ crystals heated between 1173 and 1373 K for 2 hr. Diffuse circles and streaking indicating the transition state are visible. Note the maxima in the diffuse circles along $\bar{g}(111)$ and in (c) the additional intensity besides the (drawn) diffuse circles. From (a) to (c) the indicated reflection (typical for spinel) disappears completely. Indices refer to a rocksalt-type unit cell. (d) A ⟨110⟩ reciprocal lattice section of an ill-defined $CdHo_2S_4$ crystal. Note that there are no maxima in the diffuse circles.

reflection indicated by the arrow is typical for spinel and can be compared with the reflection in Fig. 1a. The intensity of this reflection is lower than the intensity of the corresponding reflection in Fig. 1a. In the following diffraction patterns the intensity gradually becomes zero (Figs. 2b and c). What remains is diffuse intensity besides the NaCl-type reflections. At the same time the lattice parameter slightly increases from 5.69(3) to 5.72(3) Å, respectively, for Figs. 2b and c. The diffuse scattering is typical for the end of the transition from spinel to rocksalt structure. Diffuse lines run along the equivalent directions $\bar{g}(111)$. Around each basic spot the diffuse lines go into diffuse circles; the most intense are those around the (111) reflections. In most cases there are distinct maxima (satellites) in the diffuse circles in the direction $\bar{g}(111)$. Some rather ill-defined crystals, however, show no maxima in the diffuse circles (Fig. 2d). Using only the maxima a splitting $G/\Delta G = 10.3(2)$ is measured for the diffraction patterns of Fig. 2. In Fig. 2c extra intensity besides the radius of the diffuse circle is observed and also weak maxima modulating the intensity of the streaks. In order to examine the intensity around the transmitted beam additional images were recorded using a much longer cameralength. Around the transmitted beam, in only one case very weak diffuse maxima could be detected.

The ⟨111⟩ and ⟨100⟩ reciprocal lattice sections (Figs. 3a and b, resp.) show satellites without diffuse circles, which are most clear around the high-order reflections. Obviously they appear to be due to the spreading of the maxima and to the curvature of the Ewald Sphere. The reciprocal lattice sections show that there are a total of eight satellites (maxima) orientated cube-like around each Bragg reflection. In the ⟨111⟩ reciprocal lattice section (Fig. 3a) a rather diffuse reflection at the position $(\frac{4}{3}, \frac{2}{3}, \frac{2}{3})$ also appears, which becomes sharper and stronger as the transition from spinel to NaCl type is more complete. Associated with this reflection are very weak diffuse lines, forming a triangular net (too weak to

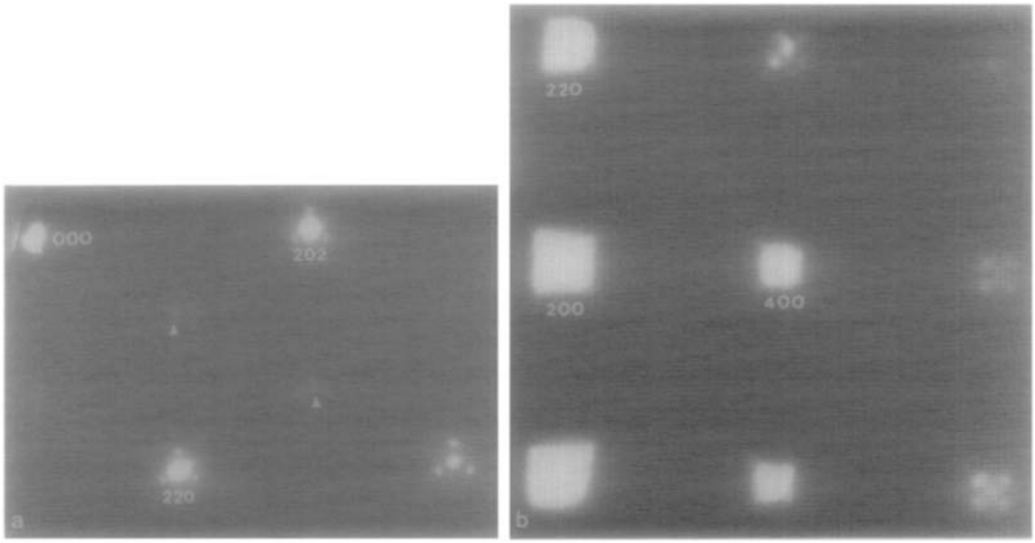

FIG. 3. (a, b) ⟨111⟩ and ⟨100⟩ reciprocal lattice sections of similarly heated $CdHo_2S_4$ crystals. Satellites become visible around the high-order reflections. The $a_h\,(3)^{1/2}$ superreflection in the ⟨111⟩ section is indicated. Indices refer to a rocksalt-type unit cell.

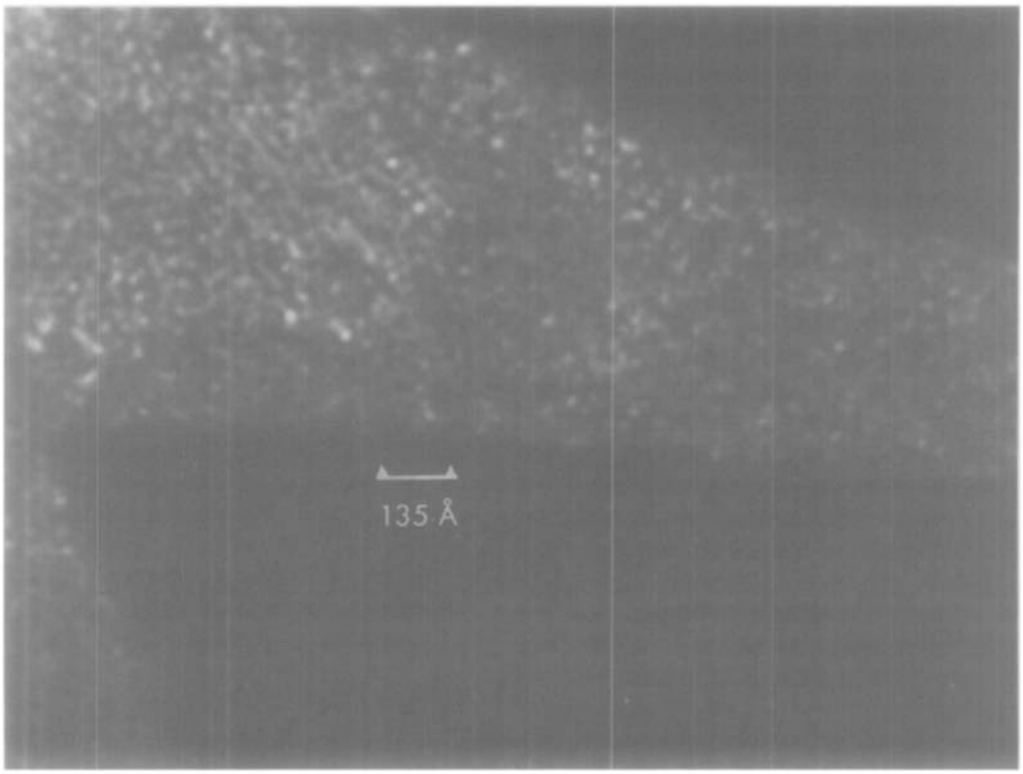

FIG. 4. Dark-field image obtained using a $(111)_{NaCl}$ reflection in a ⟨110⟩ reciprocal lattice section. Circular domains are 20 Å in size.

reproduce on the print). A dark-field image, Fig. 4, obtained using a (111) reflection from the ⟨110⟩ section (Fig. 2c) shows a domain texture. The domains are approximately 20 Å in size and are circular in shape. Note that there is only poor alignment between the domains.

3. Sample heating: T = 1173 K for 24 hr. Bright-field images obtained from these samples show that the domains tend to align in rows (Fig. 5), while size and shape do not change (compared to Fig. 4). In the corresponding diffraction pattern (Fig. 6) new first- and second-order maxima are now visible (compare the additional intensity in Fig. 2c). Other lattice sections (like the ⟨100⟩ and ⟨111⟩) indicate that the original satellites are still present under the new maxima, while the new maxima along $\bar{g}(111)$ do not appear in these sections.

Satellite Reflections

The type of satellite observed in the diffraction patterns described in the previous section is also observed in some alloy systems, for example, Au–Ni (*11*) and Cu–Ni–Fe (*12, 13*). The structural features associated with this diffraction effect are known as "spinodal decomposition" (*14*). In the spinodal region of decomposition small volumes of a second phase tend to align along certain "soft directions"[2] in the structure of the alloy. This means, in the case of the Cu–Ni–Fe alloy, for example, the formation of alternate Cu-rich and Cu-

[2] Distortions usually occur in the so-called crystallographic "soft" directions. This is determined by the elastic moduli. In cubic crystals there are three independent moduli: C_{11}, C_{12}, and C_{44} (*21*). The sign of $2C_{44} - C_{11} + C_{12}$ determines the distortion direction.

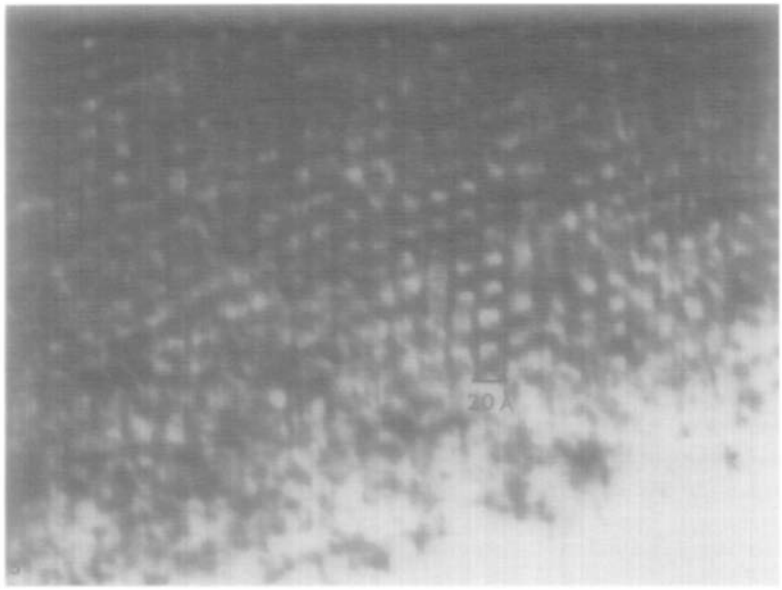

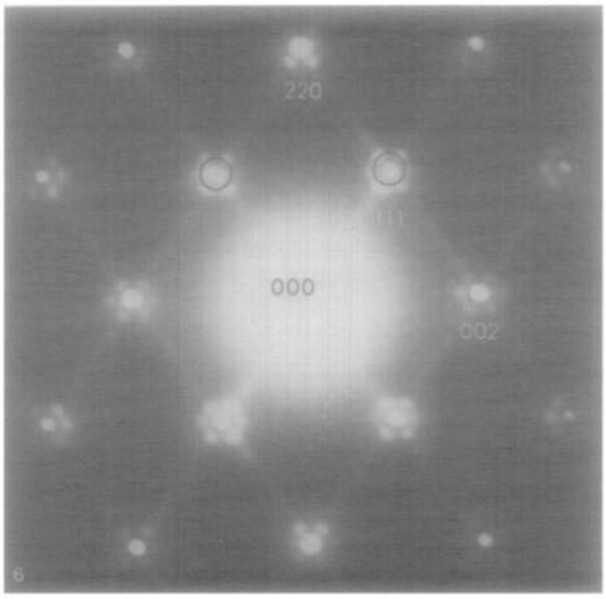

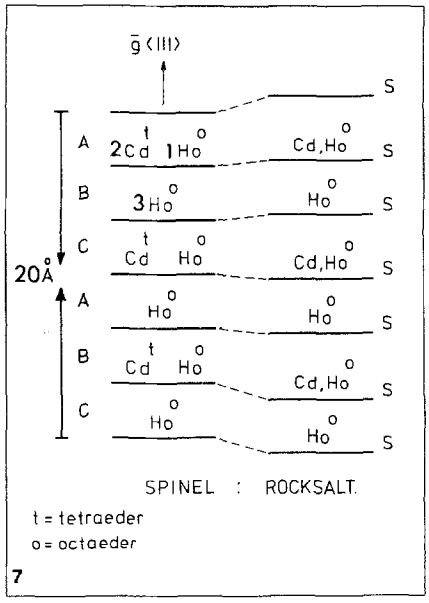

FIG. 5. Bright-field image from a $CdHo_2S_4$ crystal heated 24 hr at 1173 K. Domains of 20 Å are aligned in rows.

FIG. 6. Corresponding reciprocal lattice section. First- and second-order reflections due to cation ordering appear above the satellites of the lattice distortion. Indices refer to a rocksalt-type unit cell. The drawn circles represent the shape of the original diffuse circles like in Fig. 2.

FIG. 7. Schematic representation of sulfur layers and cations in both spinel-type structure and rocksalt-type structure.

poor lamellae, and of larger and smaller lattice spacing. When coherency is retained the result is a periodic modulation of the matrix. It is believed that this state proceeds the usual process of nucleation and growth.

The early analysis of this type of satellite showed that the modulation can be described by a regular variation of scattering factor or of lattice spacing (*15, 16*). It failed in the description of the satellite intensity because a wrong periodic function, describing the new crystal periodicity, was used. The formulation of a rectangular-shaped (rather than sinusoidal) periodic function, in conformity with the structural aspects, made it possible to give a more adequate description of the satellite intensities (for example, the intensity of first- and second-order satellites as a function of the ratio-distorted to -undistorted matrix) (*17*). Using this theory it is possible to derive the direction and wavelength of the modulation vector from the position of the satellites. In the expression for the wavelength λ_{hkl},

$$\lambda_{hkl} = \frac{a_0 \cdot h}{h^2 + k^2 + l^2} \cdot \frac{G(hkl)}{\Delta G}, \qquad (1)$$

$G(hkl)$ is a reciprocal lattice vector in direction (hkl), ΔG is the spot splitting, a_0 the lattice parameter and h the order of the reflection. From the equations for the satellite intensity it follows that the scattering contribution from the variation in scattering factor is weak compared to the contribution from the variation in lattice spacing. The contribution to the satellite intensity around the transmitted beam due to the variation in lattice parameter is zero, and the contribution from scattering factor is not zero. As it is difficult to record exact intensities in the electron microscope, only the location of the satellites will be used to find the microstructure for the compound $CdHo_2S_4$ during and after the transition from "spinel" to "rocksalt" structure.

Discussion

The electron microscopy and X-ray diffraction results confirm the existence of a spinel-type structure for $CdHo_2S_4$ below 1173 K. Samples of $CdHo_2S_4$ heated above this temperature (Fig. 2) indicate the occurrence of a "transition state."[3] At approximately 1273 K CdS evaporation is so drastic that the compound $CdHo_4S_7$ is formed. From the distribution of the diffuse scattering it is possible, using the theory described under "satellite reflections," to obtain information on the transition state structure of $CdHo_2S_4$. Later, this information will be used to discuss the low-temperature results.

The diffraction patterns of Fig. 2 show that the spinel-type structure at high temperature gradually transforms into a rocksalt-type structure. Diffuse scattering is indicative for a nonrandom distribution of Cd^{2+}, Ho^{3+}, and vacancies over the octahedral sites. The correlation does not seem to be due to coulombic interactions. Such interactions would most likely produce "clusters" (compare observations in the system $MnS-Y_2S_3$ (*18*)). However, the diffuse scattering distribution in the ⟨110⟩ sections of $CdHo_2S_4$ cannot be described using the "Cluster theory" (*19*).

On transition of spinel structure into rocksalt structure the Cd^{2+} cations have to move from a tetrahedral to an octahedral site. Comparison of the radii for 6-coordination for Cd^{2+} and Ho^{3+}, r = 1.09 and 1.05 Å, respectively (*20*), shows that Cd^{2+} is slightly larger than Ho^{3+}. Due to the dimensions of the octahedral interstices in the matrix structure (spinel) being determined by Ho^{3+}, the sulfur lattice will have to ex-

[3] In general the "transition state" is a state of partial order in a compound which is intermediate between the SRO and the LRO states in that compound (*19*) (e.g., HT and LT structure). The transition state can exist over a wide temperature trajectory, which is often not well defined.

pand locally in order to accommodate the larger Cd^{2+} cations. When, on transition, the number of Cd in octahedra increases, this deformation is not likely to remain uncorrelated in the cubic close-packed structure of the sulfur matrix. Assuming a periodic lattice distortion due to octahedral-coordinated Cd, it is possible to explain the diffuse scattering distribution in the ⟨110⟩ reciprocal lattice sections of $CdHo_2S_4$.

In these sections, the locus of the diffuse intensity distribution around the Bragg reflections (a circle which is characterized by its radius) is related to the wavelength of the modulation of the lattice planes in a crystal. The modulation wavelength logically extends over an integral number (Q) of lattice planes with spacing $d(hkl)$. Using Eq. (1) the wavelength of the lattice modulation in each crystallographic direction can be calculated. For example, along $\bar{g}(111)$: $\lambda = 20$ Å, $Q = 6 \times d(111)$; along $\bar{g}(100)$: $\lambda = 34$ Å, $Q = 6 \times d(100)$; and along $\bar{g}(110)$: $\lambda = 24$ Å, $Q = 6 \times d(110)$. This six-layer periodicity holds for all crystallographic directions. It should be realized, however, that although the distortion field of the Cd^{2+} is unidirectional, generally not all directions in a crystal will have the same distortion energy. This feature is manifested in the nonhomogeneous distribution of the diffuse intensity over the locus (circle). As the intensity is concentrated into maxima along $\bar{g}(111)$, this direction is preferred for the distortion. In ill-defined crystals this preference will be much less. Indeed in the diffraction pattern of Fig. 2d no maxima are observed in the diffuse circles.

The fact that almost no satellite intensity around the transmitted beam could be detected[4] indicates pure lattice spacing modulation, i.e., the satellite intensity is related to a deformation of the sulfur lattice only. The deformation of the sulfur lattice in the preferred ⟨111⟩ direction is pictured schematically in Fig. 7. One set of parallel {111} sulfur layers has been drawn stacked ***A B C***. As Cd^{2+} has to expand two sulfur layers in order to fit the octahedral sites (between two layers) it can only occupy alternate octahedral layers. The alternating expansion, together with the stacking sequence, is in accordance with the observed wavelength. The same description holds for the other crystallographic directions. As the expansion will be in the order of 0.05 Å (the difference in radii for Cd and Ho), which is approximately 1.5% of the $d(111)$, the distorted sulfur layers may remain coherent with the matrix. This accounts for the observed increase in unit-cell parameter during the transition into "rocksalt." The location of Cd in the {111} planes of the rocksalt-type structure can be compared with the distribution in the spinel-type structure. In the latter tetrahedral-coordinated Cd is also located alternating between {111} sulfur layers (Fig. 7). This alternation of course holds for all four equivalent {111} layers. The transition from "spinel" to "rocksalt" can thus occur along four ⟨111⟩ (preferred) directions (i.e., giving rise to 2×4 satellites).

Then small "distortion domains" will be formed in the anion lattice. The cation distribution in these domains (Fig. 7) causes the diffuse streaking along the equivalent $\bar{g}(111)$ (Fig. 2). In Fig. 4 the disalignment of the "distortion domains" (size: 20 Å = λ) indicates that the expansion in a specific direction extends only over a few sulfur layers. Moreover, the intensity of the separate domains shows that the preference of the distortion along $\bar{g}(111)$ is not yet promi-

[4] It is not possible to establish whether the very weak maxima that were detected around the transmitted beam, in just one diffraction pattern, come from double diffraction or from a modulation in scattering factor. In case of scattering factor variation, the contribution to the scattering around other Bragg reflections is very small compared with that of a variation in lattice spacing.

nent. A bright-field image taken from a crystal that was annealed for 24 hr indicates that the "distortion domains" tend to align (Fig. 5). The observed contrast is due to the modulation of the sulfur layers, mostly along $\bar{g}(111)$, extending now over many layers. At the same time the cation domains have become larger. Accordingly, in the corresponding diffraction pattern (Fig. 6), apart from the satellites from the anion lattice, broad first-order superlattice reflections appear around the Bragg reflections due to a layer-like ordering of the cations in the domains with a periodicity which is six times the $d(111)$ (Fig. 7).

Some information concerning the cation ordering within the separate {111} layers can be obtained from the ⟨111⟩ reciprocal lattice section (Fig. 3a). The superreflection indicates a 1:2 octahedral ordering (i.e., referring to a hexagonal unit cell: a a_h $(3)^{1/2}$ super cell), which suggests that in the layers containing only Ho^{3+} there exists an ordering of two Ho^{3+} and one vacancy over the octahedral sites (cf. the ordering of Al^{3+} in corundum, Al_2O_3). The ordering in this layer has then changed from a 3:1 Ho: vacancy ordering (in "spinel" before the transition to a 2:1 Ho: vacancy ordering (in "rocksalt" after the transition). This implies a movement of Ho atoms toward this layer during transition. The layers above and below this Ho/vacancy layer then contain Cd, Ho, and vacancies in a ratio 3:2:1 (note that the ratio Ho:(Cd + vacancy) = 1:2, also in agreement with the occurrence of the a_h $(3)^{1/2}$ superreflection). As the spinel superreflection completely disappears (no 3:1 ordering) and no additional reflections are observed, it seems that the Cd are distributed randomly over the octahedral sites within the {111} sulfur layers. It is not possible to conclude whether the diffuse scattering in Fig. 6 is due to a partial ordering of Cd^{2+} and Ho^{3+} and vacancies or not.

Crystals in the low-temperature region have a normal spinel-type structure according to the diffraction patterns in which no diffuse scattering or superreflections are detected. The inhomogeneous contrast and the small domains in thin crystal regions (Fig. 1b) can be explained using the high-temperature results. Extrapolation of these results suggests that the microdomains are "rocksalt-type" inclusions (in which the sulfur matrix is modulated) and that the contrast is due to strain from low concentrations of Cd in octahedral sites distributed uncorrelated within the sulfur matrix.

Conclusion

From the location of the satellites in the diffraction patterns of $CdHo_2S_4$ crystals a model could be derived that describes the structural transition from "spinel" to "rocksalt." During this transition the Cd^{2+} and Ho^{3+} cations are shifted, resulting in a structure with a distorted sulfur lattice (modulated along $\bar{g}(111)$ and with Cd and Ho occupying only octahedral sites). The observations suggest a 2:1 Ho: vacancy ordering within the octahedral {111} layers. Due to the symmetry of the basic structure, domains of the new structure will occur in the matrix corresponding to four orientation variants. The actual structure of the "rocksalt-type" domains can be compared with the structure of $CaHo_2Se_4$ (*22*) (space group $R32$, $a = 7.193(5)$ Å $= 33.08(2)°$; hexagonal cell: $a = 4.09$ and $c = 20.33$ Å). The structure can be described as a distorted rocksalt structure (elongation along the threefold axis.) in which the cations occupy octahedral sites between the sulfur {111} layers, stacked *ABC*. These layers are alternately occupied by 0.5 Cd^{2+} +0.5 vacancy and by Ho^{3+} (completely filled). The results for $CdHo_2S_4$ (H.T.) suggest that in this compound a different type of cation ordering may be considered.

The reported "intermediate" spinel-type

structure for $CdHo_2S_4$ (*8*) (X-ray diffraction) shows a close resemblance with the structure of this compound in the transition state as observed by means of electron microscopy/diffraction: domains of a new structure are growing within the matrix of the old structure. Now the mentioned occupation parameter for Cd^{2+} (see Introduction) can be interpreted in a proper way: 60% spinel-type structure (Cd in tetrahedra) plus 40% rocksalt-type structure (Cd in octahedra), which occur as domains in the spinel-type structure. This domain formation explains very well the increase in lattice parameter for this compound (*8*), as in these domains the sulfur lattice has expanded (i.e., modulation along $\bar{g}(111)$).

The stability of the spinel structure toward this new rocksalt-type (HT) structure for $CdHo_2S_4$ is determined by whether the new structure can grow coherently within the spinel-type structure (if the sulfur lattice can remain intact). Coherency, which is a very sensitive structural parameter, is thus related to the difference in radii of the two cations in this compound. Preliminary electron microscopy results on the compound CdY_2S_4 (Y^{3+} has almost the same radius as Ho^{3+}) show that the described transition also occurs in this compound. Using the difference in cation radii for spinel-type compounds AB_2S_4, it seems possible, on the basis of the criterium $(r_A - r_B) \leqq 0.05$, to predict structural instabilities (of the type described in this paper) for other spinel-type compounds.

Acknowledgment

We would like to thank Dr. D. J. W. IJdo for his helpful discussion.

References

1. O. MULLER AND R. ROY, "The Major Ternary Structural Families" (R. Roy, Ed.), p. 38–55, Springer-Verlag, Berlin (1974).
2. J. FLAHAUT, *in* "Progress in the Science and Technology of the Rare Earths" (L. Eyring, Ed.), Vol. 3, p. 236, Pergamon, New York (1968).
3. L. PAULING, "The Nature of the Chemical Bond," 3rd ed., p. 547, Cornell Univ. Press, Ithaca, N.Y. (1971).
4. A. TOMAS, I. SHILO, AND M. GUITTARD, *Mater. Res. Bull.* **13,** 857 (1978).
5. F. L. CARTER, *J. Solid State Chem.* **5,** 300 (1972).
6. L. BEN-DOR AND I. SHILO, *J. Solid State Chem.* **35,** 278 (1980).
7. W. M. YIM, A. K. FAN, AND E. J. STOFKO, *J. Electrochem. Soc.* **120,** 441 (1973).
8. H. FUJII, *J. Sci. Hiroshima Univ. Ser. A Math. Phys. Chem.* **36,** 67 (1972).
9. C. ADOLPHE, *Ann. Chim.* **10,** 271 (1965).
10. M. BAKKER AND B. G. HYDE., *Philos. Mag.* **38,** 615 (1978).
11. J. E. WOODILLA AND B. D. AVERBACH, *Acta Metall.* **16,** 255 (1968).
12. E. P. BUTLER AND G. THOMAS, *Acta Metall.* **18,** 347 (1970).
13. G. THOMAS, *in* "Diffraction and Imaging Technics in Materials Science" (S. Amelinckx, R. Gevers, and J. van Landuyt, Eds.), Vol. 1, North-Holland, Amsterdam (1978).
14. J. W. CAHN, *Trans. Metall. Soc. AIME* **242,** 166 (1968).
15. V. DANIEL AND H. LIPSON, *Proc. R. Soc. Ser. A* **181,** 368 (1943).
16. V. DANIEL AND H. LIPSON, *Proc. R. Soc. Ser. A* **182,** 378 (1944).
17. M. E. HARGREAVES, *Acta Crystallogr.* **4,** 301 (1951).
18. M. BAKKER AND C. M. PLUG, *J. Solid State Chem.* **37,** 49 (1981).
19. R. DE RIDDER, G. VAN TENDELOO, D. VAN DYCK, AND S. AMELINCKX, *Phys. Status Solidi A* **38,** 663 (1976).
20. R. D. SHANNON AND C. T. PREWITT, *Acta Crystallogr. Sect. B* **25,** 925 (1969).
21. A. J. DEKKER, "Solid State Physics," pp. 78, Macmillan, New York (1971).
22. C. SOULEAU, M. GUITTARD, AND P. LARUELLE, *Bull. Soc. Chim. Fr.*, 9 (1969).